An X-band parabolic antenna based on gradient metasurface

Cite as: AIP Advances **6**, 075013 (2016); https://doi.org/10.1063/1.4959579
Submitted: 25 March 2016 • Accepted: 11 July 2016 • Published Online: 19 July 2016

Wang Yao, Helin Yang, Xiaojun Huang, et al.

An X-band parabolic antenna based on gradient metasurface

Wang Yao,[1] Helin Yang,[1,a] Xiaojun Huang,[1,2] Ying Tian,[1] and Linyan Guo[1]
[1]*College of Physical Science and Technology, Central China Normal University, Wuhan 430079, China*
[2]*College of physics and electrical engineering, Kashgar University, Kashgar, 844000, China*

(Received 25 March 2016; accepted 11 July 2016; published online 19 July 2016)

We present a novel parabolic antenna by employing reflection gradient metasurface which is composed of a series of circle patches on a grounded dielectric substrate. Similar to the traditional parabolic antenna, the proposed antenna take the metasurface as a "parabolic reflector" and a patch antenna was placed at the focal point of the metasurface as a feed source, then the quasi-spherical wave emitted by the source is reflected and transformed to plane wave with high efficiency. Due to the focus effect of reflection, the beam width of the antenna has been decreased from 85.9° to 13° and the gain has been increased from 6.5 dB to 20.8 dB. Simulation and measurement results of both near and far-field plots demonstrate good focusing properties of the proposed parabolic antenna. [http://dx.doi.org/10.1063/1.4959579]

I. INTRODUCTION

In recent years, it has been shown that artificial controls of electromagnetic (EM) waves can be achieved by utilizing metasurfaces.[1,2] Due to the advantages of smaller geometrical dimensions and less lossy structures than bulk metamaterial, metasurfaces have originated great potential utilizations in both microwave and optical frequencies.[3,4] Typically, in the optical frequencies, the shaping of the wave front of light with optical components such as lenses and prisms, as well as diffractive elements such as gratings and holograms, relies on gradual phase shifts accumulated along the optical path.[5,6] Analogously, the new methods to control the microwave fronts are attained by introducing abrupt and gradual phase shift structure to modify the wave-path.[7,8] The phase gradient metasurface can make sense of controlling the electromagnetic waves like those optical components. Flat lenses, mirrors and axicons at telecom wavelengths based on plasmonic metasurfaces have been submitted in recent references.[9,10]

Since high-gain antenna is a necessary device for the long distance wireless communication system, quite a lot of attention has been attached on the exploration of new techniques for improving it. Methods have been taken to improve the antennas' gain such as antenna arrays,[11,12] horn antenna,[13] leaky wave antenna,[14] lens antenna,[15–17] and reflector antenna.[18–20] Conventional antenna arrays always require complex feed network to realize high gain.[21,22] Horn antennas have the superiority of high-gain and wide bandwidths but they are too bulky.[23] Leaky wave antennas can generate high gain within a low profile while they typically suffer from narrow bandwidths.[24,25] Lens antennas based on metamaterials are the emerging ideas for the high-gain antenna schemes. However, the design of the transmitting meta-lens is difficult since the transmitting efficiency must be taken into consideration.[15,16] The reflector antenna such as parabolic antenna has been used for a long time. A typical parabolic antenna consists of a metal parabolic reflector with a small feed antenna dangled in front of the reflector at its focus, pointed back toward the reflector.[19] The reflector is a metallic surface formed into a paraboloid of revolution and usually truncated in a circular rim that forms the diameter of the

[a]emyang@mail.ccnu.edu.cn

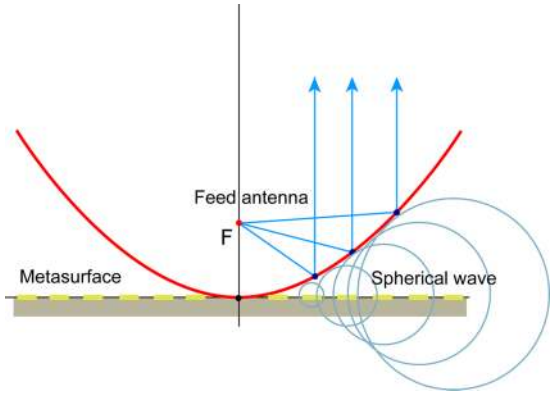

FIG. 1. The schematic of the proposed parabolic antenna.

antenna.[26] However such a parabolic reflector has the drawbacks of large profile and hard fabrication. More recently, two dimensional (2D) metasurfaces were adopted to achieve phase modulation in an ultrathin layer. Yu *et al*. used a plasmonic nanoantenna array consisting of V-shaped gold to introduce phase discontinuity at the bounding surface.[5] Both anomalous reflection and refraction are demonstrated to control and focus the electromagnetic waves, followed by various designs using different approaches.[3,10,27] Compared with the transmitting gradient metasurface the reflecting gradient metasurface is easier to get high reflectivity than the transmittance.[28,29] Thus we can take place of the traditional metal parabolic reflector by the properly designed metasurface utilizing the phenomenon of anomalous reflection.[30]

In this work, we propose a gradient metasurface reflector which can reflect and focus the diffuse electromagnetic waves. The reflector has a parabolic phase profile at 10 GHz. The red curve in the schematic of Fig. 1 follows the parabolic profile and it signify where has the same phase shift due to the anomalous reflection. A low-gain patch antenna locates the focus of the parabolic profile as the feed of the parabolic antenna. The quasi-spherical wave emitted by the source will be transformed to the near-plane wave and reflect to the reverse orientation by the reflector. Thus a high-gain antenna with a narrow main lobe along the antenna's axis will be achieved.

II. REALIZATION OF THE ANOMALOUS REFLECTION

The basic unit of metasurface is a sub-wavelength circle patch on a grounded dielectric substrate, as shown in Fig. 2, in which the gray and orange areas are dielectric and metal. The period of square lattice is $a = 10mm$, and the radius of the solid circle patch varies from 3.4 to 4.4 mm. Rogers RO4003 is chosen as the dielectric substrate with the dielectric constant 3.38 and the thickness 1.524 mm. The dispersion curves with changing radius of the patches also shown in Fig. 2, and the radius of the circle patches determines the value of surface impedance. Surface impedance dispersion curves reveal the phase shift when front waves reflected by the unit metasurface with corresponding radius. When slowly varying the radius in the simulation to obtain different surface impedances, the metasurface could have gradient phase shift and shows anomalous refraction and reflection.

In order to validate the fact that the phase gradient metasurface which has the phase shifts range from 0 to 2π with high reflection efficiency can present anomalous reflection, we propose a super cell composed of seven elements and each element's radius have been shown in Fig. 3. The figure also describes the simulated reflection phase shift and amplitude of these seven cells at 10 GHz. The discrete phase shift of each cell is arranged in steps of $\pi/4$. It's remarkable of all the reflection amplitudes are approaching 1.

The anomalous reflection effect can be explained by the generalized reflection law, and following is the formula of the law:

$$\sin\theta_r - \sin\theta_i = \frac{\lambda}{2\pi n_i}\frac{d\varphi}{dx} \tag{1}$$

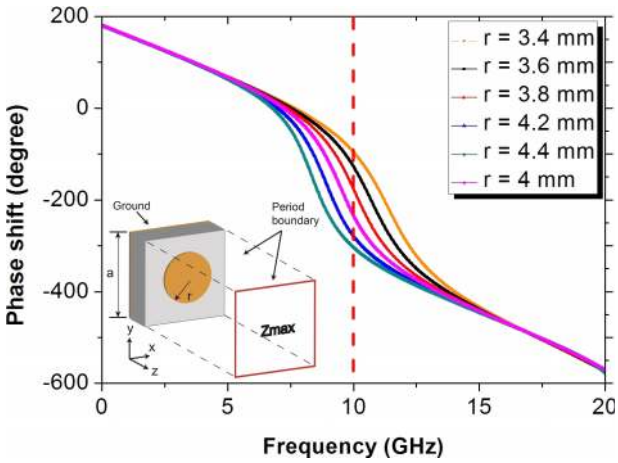

FIG. 2. The basic unit of the metasurface and the phase shift dispersion curves of unit cells with different radius values. The red dotted line is target frequency.

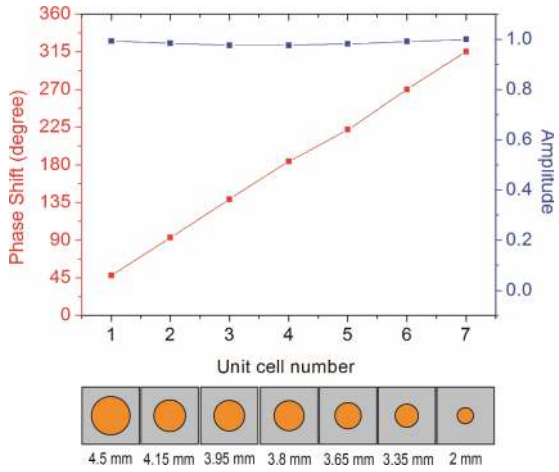

FIG. 3. Simulated reflection phase shift (blue dots) and amplitude (red dots) of unit cell with different radius of the solid circle r at 10 GHz.

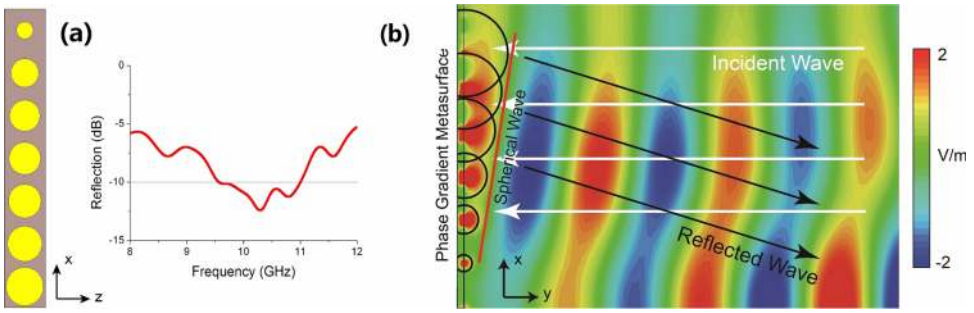

FIG. 4. The seven cells to verify the anomalous reflection, (a) the reflectivity of the seven cell (b) the electric field distribution of the reflection at 10 GHz.

in which φ is the phase shift at a regional position on the metasurface, n_i is the refractive index of the incident medium, θ_r (θ_i) is the reflected (incident) angle of the electromagnetic wave, λ is the wavelength, and we can get $d\varphi/dx = \pi/4a$ from the super cell's structure, where a is the period of square lattice. Since the reflex phenomenon occurs in free space ($n_i = 1$) the θ_r can be obtained by

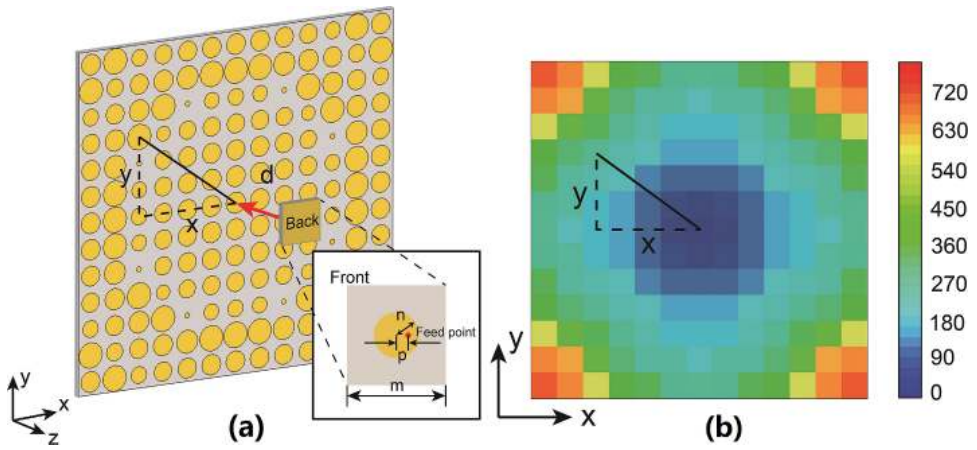

FIG. 5. (a) The designed patch antenna loaded on the gradient metasurface. (b) Phase distributions and focusing effect of the proposed design.

FIG. 6. Fabrication of the patch antenna and the gradient metasurface.

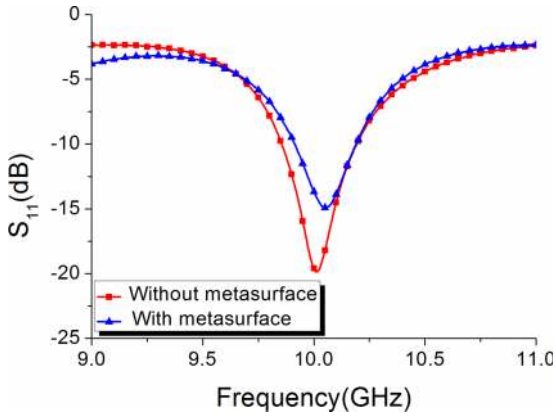

FIG. 7. Measured return losses of the patch antenna and with the designed gradient metasurface.

$$\theta_r = \arcsin\left(\frac{\lambda}{2\pi} \times \frac{\pi}{4a}\right) \tag{2}$$

By substitution of $\lambda = 3a$ ($f = 10GHz$) into the equation above, $\theta_r = 22°$ is the theoretical calculation result. The super cell to validate anomalous reflection caused by the phase gradient metasurface is shown in Fig. 4. The figure also demonstrates the simulated the reflectivity of the surface and the electric field distribution in *xoy*-plane at 10 GHz by CST MICROWAVE STUDIO. A plane wave income to the surface vertically and the z-axis is periodic boundary. Fig. 4(a) shows the reflectivity at 9.5 ~ 11 GHz is below -10 dB, that means the anomalous reflection occurred in the band. When

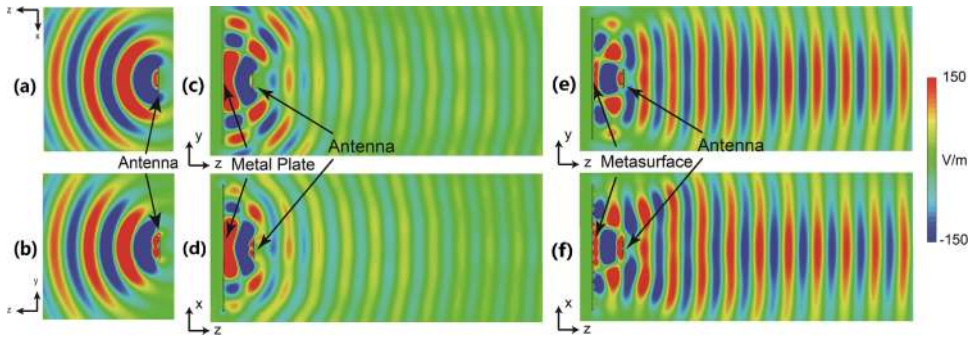

FIG. 8. Simulated electric field distributions at 10 GHz in *xoz*-plane and *yoz*-plane, respectively, for the patch antenna are shown in (a) and (b) the reflected wave by the metal plate are (c) and (d) the reflected wave by the designed gradient metasurface are (e) and (f).

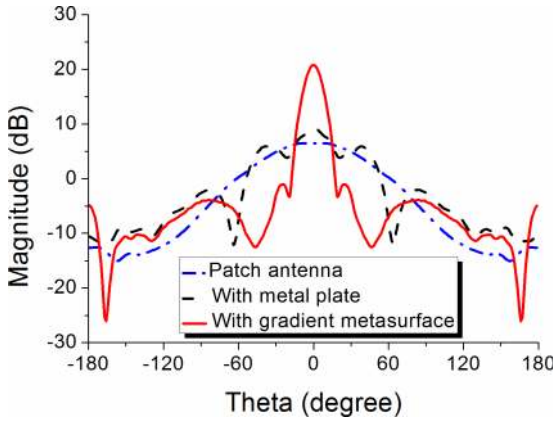

FIG. 9. Comparison of the simulated *yoz*-plane radiation patterns of the patch antenna and with two different reflectors.

the incident plane waves vertically irradiate the metasurface, each patch on the surface can activate spherical waves with different radius since the phase shifts of each units are different. The same phase plane can be sloping plane if the phase shifts change lineally. It is observed from the Fig. 4(b) that the reflection wave deflects to the $-x$ direction (phase delay direction) with the angle approximately equal to the theoretical value 22°.

III. DESIGN OF THE PARABOLIC ANTENNA

The parabolic reflector has the property of focusing the wave propagating along its paraxial direction, which can be applied to design the high-directive antenna. To achieve planar focus reflector, the reflected phase shift distribution in *xoy*-plane should follow the parabolic profile:

$$\varphi(x, y) = \frac{2\pi}{\lambda}\left(\frac{x^2 + y^2}{4f}\right) + \varphi_0 \tag{3}$$

in which f is the focal distance, φ_0 is the phase shift by the reflection of the first unit cell placed at the point $x = 0$, $y = 0$. We particularly select $f = \lambda = 30mm$ so that 7 unit cells can cover $0 \sim 2\pi$ phase shift in x or y direction, the phase shift of each unit is satisfied with the parabolic profile of formula (3) in the metasurface. A patch antenna is placed at the focal point ($d = f$) and it radiates toward the metasurface as indicated in Fig. 5(a). The patch antenna adopts circular radiation patch and it feed by a 50Ω SMA at the proper position marked in the figure. The radius of the patch is $n = 4.3mm$ and the feed point is $p = 2.2mm$ apart from the center. The two-dimensional phase shift distributions of

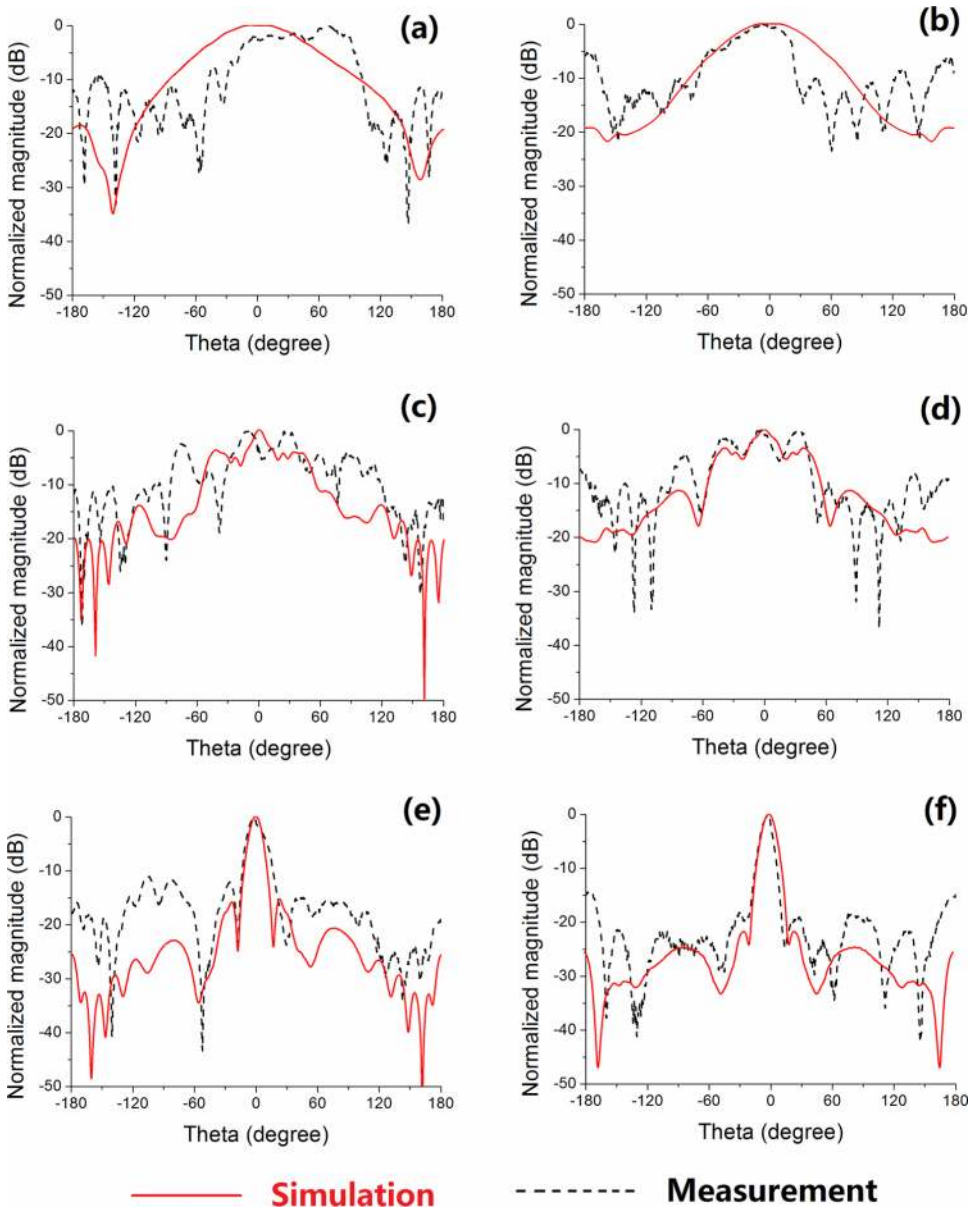

FIG. 10. Comparison of the simulated and measured radiation patterns of three antennas. The *xoz*-plane and *yoz*-plane radiation patterns: (a), (b) are the designed patch antenna; (c), (d) are the antenna with metal plate; and (e), (f) are the antenna with the designed gradient metasurface.

the gradient metasurface are shown in Fig. 5(b). For the unit cell shown in the figure, $x = 4$, $y = 3$, the corresponding phase shift is 250°.

The gradient metasurface reflector and the patch antenna are fabricated and measured, as shown in Fig. 6. Fig. 7 gives the measured return loss of the proposed patch antenna and the parabolic antenna. An Agilent E8362B network analyzer was used to measure the return loss, which provides the return loss of parabolic antenna is less than -10 dB from 9.8 to 10.3 GHz, matching well with the patch antenna.

The electric field distribution of the patch antenna, metal plate reflector antenna and the parabolic antenna are shown in Fig. 8. It indicates that the gradient metasurface can reflect the quasi-sphere waves incoming from the proposed patch antenna. Compared with the divergent electric field reflected by the metal plate, the electric field reflected by proposed metasurface is intensive and the reflected

near-plane waves are high directivity. Fig. 9 shows the comparison of the *yoz*-plane radiation patterns of these three antennas at 10 GHz. Due to the focus effects of the metasurface and the high directivity of the near-plane wave, the beam width of the parabolic antenna is obviously decreased compared with the two other antennas and the gain is remarkably enhanced. The realized gain of the patch antenna is only 6.5 dB; the metal plate reflector increased the gain to 9.3 dB; the gradient metasurface enhanced the gain to 20.8 dB dramatically. From the simulation, Half-Power Beam Width (HPBW) and Side Lobe level (SLL) can also be obtained. The HPBW patch antenna is 85.9°, the antenna with metal plate reflector is 18.8°, and the parabolic antenna is 13°. The radiation pattern of patch antenna is quasi-spherical and has no side lobe, the SLL of the second antenna is -3.7 dB, and the parabolic antenna is -21.8 dB. Lower HPBW and SLL indicate the proposed parabolic antenna is outstanding high-gain antenna for long distance wireless communication system.

For further verification, the simulated and measured radiation patterns in *xoz* and *yoz*-plane at 10 GHz are illustrated in Fig. 10. In the measurement, a broadband horn antenna (1 ∼18 GHz) is employed as a receiving antenna, and the three proposed antennas are used as transmitting antennas respectively. The measurements agree well with the simulation results and small disparities are attributed to the disturbance from the experimental environment. Compared with the first two antennas, the proposed parabolic antenna shows a highly directive emission.

IV. CONCLUSION

In summary, we proposed an X-band parabolic antenna based on a gradient metasurface as "parabolic reflector" which was demonstrated to enhance the gain of antenna, and the reflected phase shift distribution in the surface follows a parabolic profile. The outstanding focusing effects of the metasurface guarantee the good performances of the parabolic antenna. The parabolic antenna has been simulated, fabricated and measured, shows desirable high-gain and low HPBW, SLL properties. The peak gain is 20.8 dB, HPBW is 13°, and SLL is -21.8 dB. Measured radiation patterns agree well with the simulation results and proved it has the excellent properties as anticipated. Thus the proposed parabolic antenna is qualified for long distance wireless communication systems.

ACKNOWLEDGEMENTS

This work was supported by the National Natural Science Foundation of China (Grant No. 41474117) and by self-determined research funds of CCNU from the colleges' basic research and operation of MOE (No.CCNU15GF005).

[1] S. Sun, K.-Y. Yang, C.-M. Wang, T.-K. Juan, W. T. Chen, C. Y. Liao, Q. He, S. Xiao, W.-T. Kung, and G.-Y. Guo, Nano Lett. **12**, 6223-6229 (2012).
[2] S. Sun, Q. He, S. Xiao, Q. Xu, X. Li, and L. Zhou, Nat. Mater. **11**, 426-431 (2012).
[3] Y. B. Li, X. Wan, B. G. Cai, Q. Cheng, and T. J. Cui, Sci. Rep. UK **4**, 6921 (2014).
[4] X. Wan, W. X. Jiang, H. F. Ma, and T. J. Cui, Appl. Phys. Lett. **104**, 151601 (2014).
[5] N. Yu, P. Genevet, M. A. Kats, F. Aieta, J.-P. Tetienne, F. Capasso, and Z. Gaburro, science **334**, 333-337 (2011).
[6] E. G. Loewen and E. Popov, *Diffraction gratings and applications* (CRC Press, 1997).
[7] X. Ni, S. Ishii, A. V. Kildishev, and V. M. Shalaev, Light-Sci. Appl. **2**, e72 (2013).
[8] N. Yu and F. Capasso, Nat. Mater. **13**, 139-150 (2014).
[9] F. Aieta, P. Genevet, M. A. Kats, N. Yu, R. Blanchard, Z. Gaburro, and F. Capasso, Nano Lett. **12**, 4932-4936 (2012).
[10] A. Pors, M. G. Nielsen, R. L. Eriksen, and S. I. Bozhevolnyi, Nano Lett. **13**, 829-834 (2013).
[11] B. Li, B. Wu, and C.-H. Liang, Prog. Electromagn. Res. **60**, 207-219 (2006).
[12] P. R. Grajek, B. Schoenlinner, and G. M. Rebeiz, IEEE Trans. Antennas Propag. **52**, 1257-1261 (2004).
[13] K. Chung, S. Pyun, and J. Choi, IEEE Trans. Antennas Propag. **53**, 3410-3413 (2005).
[14] D. R. Jackson, C. Caloz, and T. Itoh, P. IEEE **100**, 2194-2206 (2012).
[15] H. Li, G. Wang, H.-X. Xu, T. Cai, and J. Liang, IEEE Trans. Antennas Propag. **63**, 5144-5149 (2015).
[16] Y. Shi, K. Li, J. Wang, L. Li, and C.-H. Liang, IEEE Trans. Antennas Propag. **63**, 3742-3747 (2015).
[17] J. Kim, D. Shin, S. Choi, D.-S. Yoo, I. Seo, and K. Kim, Appl. Phys. Lett. **107**, 101906 (2015).
[18] W. Menzel, D. Pilz, and M. Al-Tikriti, IEEE Antennas Propag. M. **44**, 24-29 (2002).
[19] C. Cutler, P. IRE **35**, 1284-1294 (1947).
[20] L. Guo, B. Xiao, M. Li, H. Yang, and H. Lin, J. Electromagnet. Wave. **29**, 693-702 (2015).
[21] J. B. Andersen, IEEE Antennas Propag. M. **42**, 12-16 (2000).
[22] A. P. Feresidis, G. Goussetis, S. Wang, and J. C. Vardaxoglou, IEEE Trans. Antennas Propag. **53**, 209-215 (2005).
[23] A. W. Love, *Electromagnetic horn antennas* (IEEE, Press, 1976).

[24] S. Paulotto, P. Baccarelli, F. Frezza, and D. R. Jackson, IEEE T. Microw. Theory. **56**, 2826-2837 (2008).
[25] T. Zhao, D. R. Jackson, J. T. Williams, H.-Y. D. Yang, and A. A. Oliner, IEEE Trans. Antennas Propag. **53**, 3505-3514 (2005).
[26] W. L. Stutzman and G. A. Thiele, *Antenna theory and design* (John Wiley & Sons, 2012).
[27] X. Ni, N. K. Emani, A. V. Kildishev, A. Boltasseva, and V. M. Shalaev, Science **335**, 427-427 (2012).
[28] C. Saeidi and D. van der Weide, Appl. Phys. Lett. **105**, 053107 (2014).
[29] H. Li, G. Wang, J. Liang, and X. Gao, Prog. Electromagn. Res. **155**, 115-125 (2016).
[30] H. Hou, G. Wang, H. Li, T. Cai, and W. Guo, Acta Phys. Sin. **65**, 027701 (2016).